Journal of Macromolecular Science, Part A
Publication details, including instructions for authors and subscription information:
http://www.informaworld.com/smpp/title~content=t713597274

Development and Characterization of a Radio Frequency-Transparent Ablator

Eric L. Strauss[a]
[a] Martin Marietta Corporation, Denver, Colorado

To cite this Article Strauss, Eric L.(1969) 'Development and Characterization of a Radio Frequency-Transparent Ablator', Journal of Macromolecular Science, Part A, 3: 4, 735 — 761
To link to this Article: DOI: 10.1080/10601326908053838
URL: http://dx.doi.org/10.1080/10601326908053838

J. MACROMOL. SCI.–CHEM., A3(4), pp. 735-761, July, 1969

Development and Characterization of a Radio Frequency-Transparent Ablator

ERIC L. STRAUSS

Martin Marietta Corporation
Denver, Colorado

SUMMARY

Earth and planetary entry vehicles require heat shield materials whose transparency to radio frequency (rf) signals is unaffected by the ablation process. Teflon or fused silica are currently used for this purpose, but these materials are heavy and difficult to attach. For applications such as Mars entry vehicles or lifting bodies where low heating rates prevail, low-density, rf-transparent ablators are desired. To fill this need, Martin Marietta Corporation has developed a rf-transparent composition designated SLA-220. This ablator, a silica-filled elastomeric silicone, has a density of 0.25 g/cm^3 and forms a siliceous rather than a carbonaceous char. Pyrolysis of SLA-220 at slow heating yields a pure silica residue. As heating rate increases, the volatile pyrolysis products tend to undergo secondary decomposition and to deposit carbon while passing through the hot char. Therefore, rf signal attenuation increases with heating rate. Electrical properties of SLA-220 (dielectric constant, signal attenuation) have been measured before and after ablation. Ablation testing has been conducted at heating rates ranging from 6 to 60 Btu/ft^2-sec. Thermal properties (conductivity, specific heat, expansion) and mechanical properties (strength, elastic modulus, elongation) have been determined. The properties of SLA-220 are compared with those of 0.50 and 0.70 g/cm^3 porous Teflon ablators to demonstrate the advantages of SLA-220 over other low-density rf-transparent ablative systems.

INTRODUCTION

Ablation is a proven thermal protection method for earth re-entry and planetary entry vehicles. Depending on the mission objective and the resulting heat flux and pressure levels, different types of ablators can be selected. These include phenol-formaldehyde resins reinforced with silica, carbon, or nylon fibers for high heat flux, short time pulses [1], low-density charring ablators based on silicone and epoxy resins for the intermediate heating range [2], and superlight ablators for low-heating-rate, low-pressure environments [3]. In all of these systems, decomposition of the resin and of organic fillers yields a carbon-containing char. Surface recession in chars containing a high percentage of silica fiber and microsphere fillers is generally attributable to melting, while oxidation is the dominant surface recession mechanism in chars composed largely of carbon fibers in a carbonaceous residue matrix. Ablators with high silica content whose surface temperature does not exceed the melting point of silica during ablation will exhibit little or no surface recession.

Many entry and re-entry missions require transmission of radio frequency signals while the vehicle passes through the atmosphere [4]. Signal transmission may be necessary to facilitate communication, guidance and control, radar altimeter operation, or data transmittal. Since the carbon chars of conventional ablators prevent signal transmission, special heat shield materials must be employed. In the past, selected materials have generally fallen into one of two categories: (a) subliming ablators such as Teflon, or (b) refractory nonmetallics such as fused silica or boron nitride. The disadvantages of these materials are associated with their high density and relatively high thermal conductivity; consequently, their ablative efficiencies tend to be low. In addition, the poor bonding characteristics of Teflon and the brittle nature of the ceramics make these materials difficult to attach. The general design approach utilized windows of a rf-transparent ablator, framed by edge members, and set in a conventional ablative heat shield. For applications where low-density charring ablators or superlight ablators (e.g., Martin Marietta SLA-561 [5]) are employed, it is desirable to use rf-transparent ablators whose density, thermal conductivity, and ablation characteristics are more closely matched with those of the primary heat shield material than are those of fused silica or Teflon. Various material concepts have been investigated as potential low-density, rf-transparent ablators, including porous Teflon, foamed silica, and a network of sintered silica fibers [6].

Martin Marietta undertook the development and evaluation of

rf-transparent ablators as part of its heat shield research program for a Mars lander. The selected approach involved the use of an elastomeric silicone matrix with silica, in either fiber and/or hollow microsphere form, as the only filler material. Porous Teflon was selected as the comparison standard since Teflon has been employed as an ablating antenna window material in numerous flight vehicles (e.g., Ref. [7]). The optimum density of a porous Teflon ablator for the Mars entry environment was not known; consequently, procedures for producing porous Teflon at three controllable density levels (0.50, 0.60, and 0.70 g/cm^3) were developed as part of this program.

In the initial phase of the ablator development program, material samples were formulated and subjected to heating by means of a propane torch or quartz lamp radiation. Char formation was observed and char depths were measured. Compositions which did not develop a dense carbon char were then screened for electrical properties. Measurements were taken of dielectric constant and loss tangent on both charred and uncharred samples. The criterion for suitability as rf-transparent ablator was that charring produce only small changes in the dielectric constant and loss tangent of the material.

On the basis of these screening tests, a 0.25-g/cm^3-density silica-filled silicone elastomer was selected for further evaluation as a rf-transparent ablator. The material has been designated SLA-220. Radio frequency transparency, ablative efficiency, mechanical properties, thermal properties, and weight loss characteristics have been measured and are discussed in subsequent sections of this paper. In many instances, the performance of SLA-220 is compared with that of porous Teflon and also with that of SLA-561, a Martin-Marietta-developed superlight ablator of 0.225 g/cm^3 density. SLA-561 is a high-efficiency ablative composition and develops a carbon char during ablation; consequently, it is not suitable as a rf-transparent ablator. However, it does provide a basis of comparison for evaluating the thermal, mechanical, and ablative characteristics of SLA-220.

ELECTRICAL PROPERTIES

Char Formation

The rf-transparent SLA-220 composition evolved from a systematic investigation of components and materials variables including type of resin, type and percentage of fillers, type and percentage of catalyst, and cure

schedules. Samples, 2.5 in. in diam, were prepared and exposed for 2 min to the flame of a propane torch to ascertain the effects of these variables on char formation. To illustrate the type of result obtained, a tested sample of SLA-220 is shown in Fig. 1 alongside a material which has the identical composition except that the amount of catalyst has been increased by 67%. The photographs show that the sample with the higher catalyst concentration developed a dark char at the point of flame impingement while SLA-220 has a uniform grey appearance.

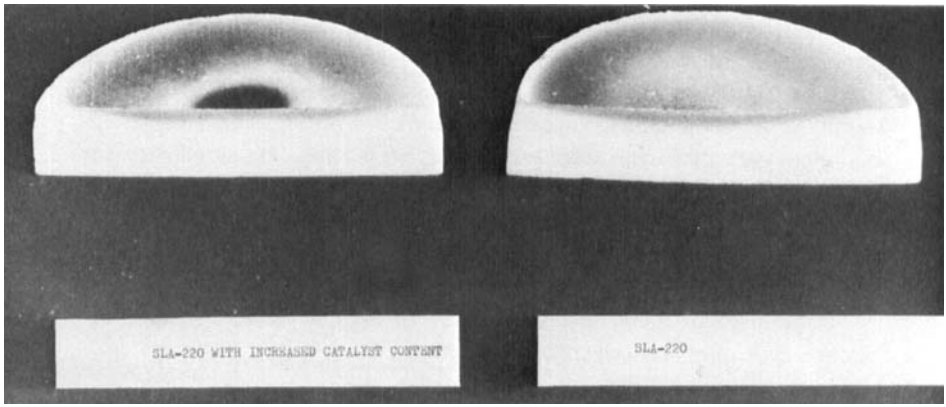

Fig. 1. Char formation of silica-filled silicone ablators heated for 2 min with a propane torch.

More detailed investigations of SLA-220 revealed that this ablator decomposes to a white SiO_2 residue (residual weight fraction, 0.72) when subjected to gradual heating in argon, as occurs in thermogravimetric analysis (Fig. 2). However, when SLA-220 is subjected to rapid heating from one side, as occurs during ablation, a darker, carbon-containing char is formed. The gaseous decomposition products formed in the pyrolysis zone of the ablating sample undergo further cracking while flowing outward through the hot char. This secondary decomposition is accompanied by deposition of small amounts of carbon in the char zone. Carbon deposition in silica-filled silicone ablators has been found to increase with increasing char temperature and, therefore, with increasing heat flux. Since rf signal attenuation appears to increase with the amount of carbon in the char, the rf-transparency of SLA-220 is a function of the intensity and duration of the heat flux to which the ablator is exposed.

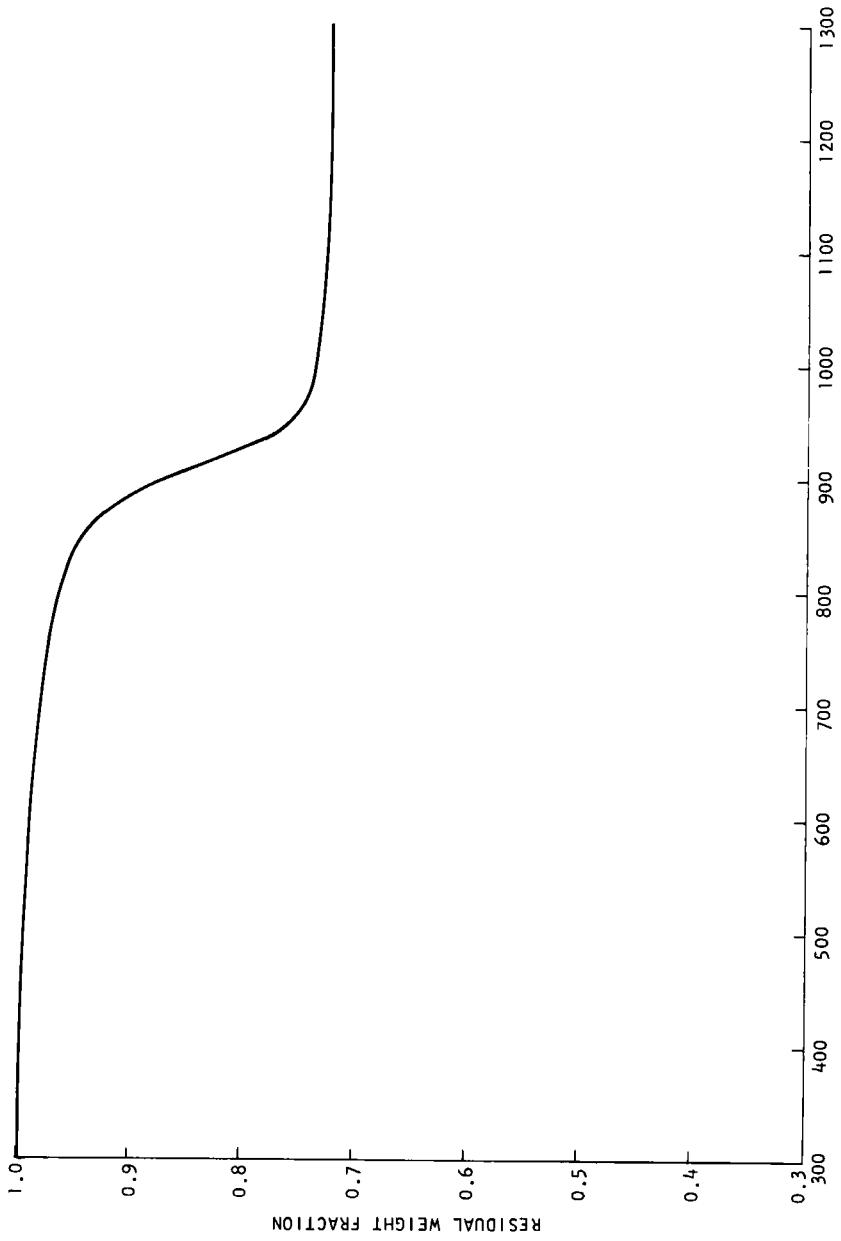

Fig. 2. Thermogravimetric analysis for SLA-220.

Figure 3 compares two samples of SLA-220, 2.5 in. in diam X 0.5 in. thick, which were charred in air under quartz lamp radiant heating. Specimen 180-2-1 was heated for a period of 95 sec at a flux level of 11.4 Btu/ft^2-sec, while sample 180-2-2 was exposed for 60 sec to 22.5 Btu/ft^2-sec. Figure 4 is a similar comparison of SLA-220 samples heated in a plasma arc. Sample 27-2 was 0.5 in. thick and was exposed for 250 sec to a heat flux of 6 Btu/ft^2-sec in a 28% CO_2-72% N_2 atmosphere. Sample 27.5 was 0.425 in. thick and had been exposed for 50 sec at 60 Btu/ft^2-sec. Results of these tests are summarized in Figs. 3 and 4. The thickness of dark char in sample 180-2-1 (11.4 Btu/ft^2-sec radiant heating) was only half that of sample 180-2-2 (22.5 Btu/ft^2-sec radiant heating). In addition, the char surface and cross section of sample 180-2-1 is light grey while that of specimen 180-2-2 is dark grey to black. Analogous charring characteristics are noted for the plasma arc-exposed samples. Specimen 27-2 (6 Btu/ft^2-sec) developed only a thin surface carbon layer while specimen 27-5 (60 Btu/ft^2-sec) has a carbon-containing char layer of appreciable thickness.

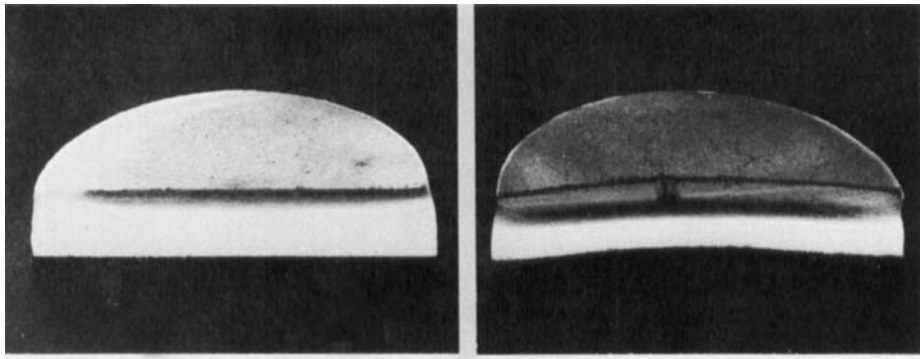

SAMPLE NO.	180-2-1	180-2-2
TYPE OF HEATING	QUARTZ LAMP	QUARTZ LAMP
FLUX LEVEL (BTU/FT^2-SEC)	11.4	22.5
EXPOSURE TIME (SEC)	95	60
CHAR DEPTH (IN.)		
DARK CHAR	0.15	0.28
WHITE CHAR	0.07	0.07
TOTAL CHAR	0.22	0.35

Fig. 3. Comparison of SLA-220 chars formed at low and high radiant heat fluxes.

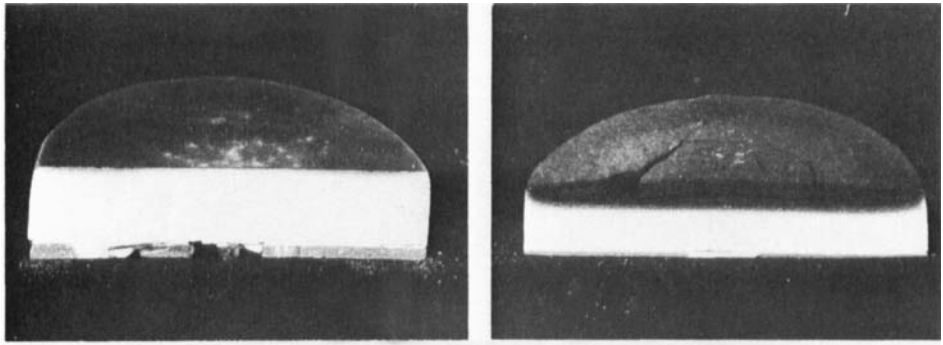

SAMPLE NUMBER	27-2	27-5
TYPE OF HEATING	PLASMA ARC	PLASMA ARC
FLUX LEVEL (BTU/FT^2-SEC)	6.0	60
EXPOSURE TIME (SEC)	250	50
CHAR DEPTH (IN.)		
DARK CHAR	0.02	0.17
WHITE CHAR	0.15	0.06
TOTAL CHAR	0.17	0.23

Fig. 4. Comparison of SLA-220 chars formed at low and high plasma arc heat fluxes.

Figure 5 shows plots of char depth vs. length of exposure for SLA-220 radiantly heated at 11.4 and 22.5 Btu/ft^2-sec. Within the range of exposure times of these tests, both total char depth and thickness of the carbon-containing char layer are shown to increase approximately linearly with time.

Radio Frequency

Electrical characteristics of charred and uncharred samples of SLA-220 were tested by means of a "shorted-line" technique wherein small samples of the ablator were fitted into a shorted-wave guide section.

Changes in the standing wave (at a frequency of 10 Kmc) were measured and analyzed to derive the dielectric constant and signal attenuation of the material. A maximum signal loss of 6 dB under the test conditions employed (two-way loss) is considered acceptable. Test results are summarized in Table 1. They indicate that SLA-220 possesses a very low dielectric constant which does not vary with charring. Signal attenuation is less than the 6 dB limit value for all heating conditions employed.

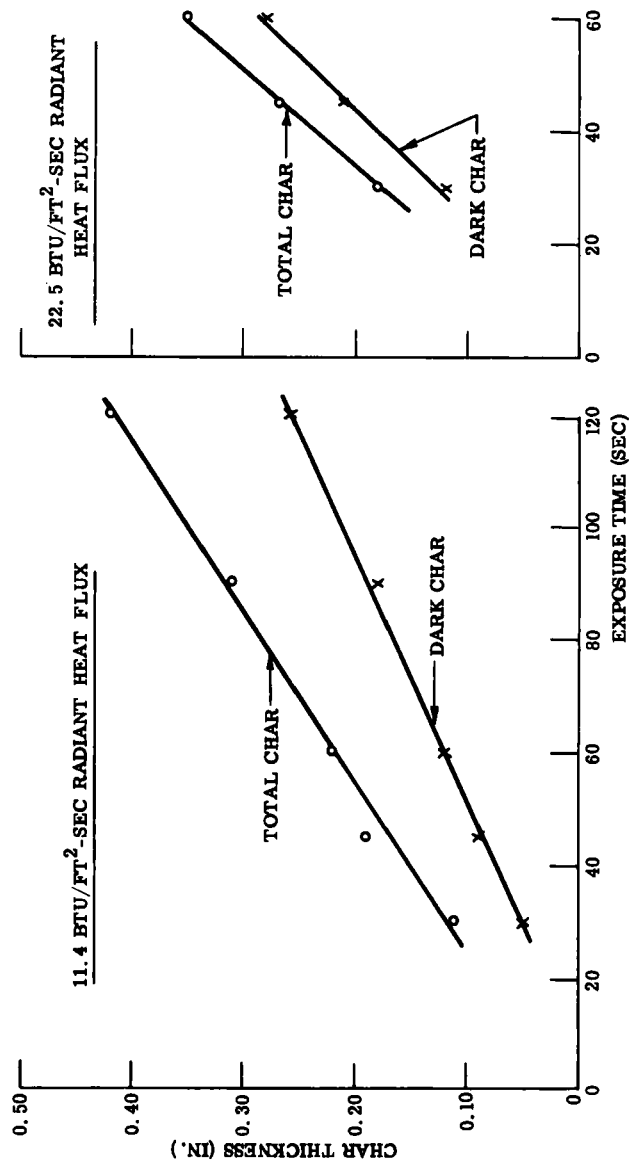

Fig. 5. Char growth with exposure time for SLA-220.

Table 1. Radio Frequency Signal Attenuation for SLA-220 Ablator

Ablator thickness, in.	Heating rate, Btu/ft^2-sec	Exposure time, sec.	Type of heating	Char depth, in.	Signal attenuation,[a] dB	Dielectric constant
0.507	–	–	–	0	0.5	1.2
0.520	11.4	45	Quartz lamps	0.22	0.8	1.2
0.509	11.4	95	Quartz lamps	0.35	1.6	1.2
0.610	22.5	60	Quartz lamps	0.33	5.5	1.1
0.554	11.4	95	Quartz lamps	0.31	0.8	1.1
0.355	6	250	Plasma arc	0.15	0.8	1.1
0.330	60	50	Plasma arc	0.24	1.6	1.1

[a]Two-way loss.

Signal attenuation increases with length of exposure at a given heating rate (i.e., 45 and 95 sec at 11.4 Btu/ft^2-sec). Exposure for 95 sec at 11.4 Btu/ft^2-sec and 60 sec at 22.5 Btu/ft^2-sec produced equivalent char thicknesses; however, signal attenuation was significantly higher for the sample subjected to the higher heat flux. Type of heating appears to have a definite influence on char formation and dB loss, as is apparent from the lack of correlation between radiantly heated and plasma arc-heated samples.

ABLATIVE EFFICIENCY

Propane Torch Screening Tests

Initial ablative screening of rf-transparent ablators was conducted with a propane torch at a heating rate of approximately 42 Btu/ft^2-sec. All samples tested were 2.5 in. in diam and were of equal weight, 0.625 lb/ft^2. To provide equal specimen weights, specimen thickness ranged from 0.167 in. for porous Teflon (ρ = 0.71 g/cm^3) to 0.526 in. for SLA-561 (ρ = 0.23 g/cm^3). Specimens were instrumented with a Chromel-Alumel thermocouple which was attached to the specimen back face, and they were bonded to a low-conductivity silicone foam to prevent extraneous heating of the back face. The test samples were exposed to the propane flame until their back face temperature rose from ambient (75°F) to 475°F. Typical results are summarized on Table 2.

Figure 6 compares back-face temperature rise of SLA-220 with that of the ablators listed in Table 2. While the back-face temperature of SLA-220 is seen to rise more rapidly than that of the high-efficiency SLA-561 ablator, SLA-220 affords greater thermal protection on an equal weight basis than porous Teflon or the MA-25s sprayable silicone ablator.

Plasma Arc Testing

Samples of Martin Marietta SLA-220 were tested in a 240-kW Plasma arc at nominal heating rates of 6 and 60 Btu/ft^2-sec and for durations of 250 and 50 sec respectively. The test atmosphere was a mixture of 28% CO_2 and 72% N_2. Test specimens were 2.5-in.-diam, flat-faced cylinders, bonded to a cast epoxy base. Back-face temperature rise was measured with a Chromel-Alumel thermocouple attached to the ablator back face by means of a 0.25-in.-diam, 2.5-mil-thick, stainless-steel disk.

Table 2. Propane Torch Test Results

Material	Density, g/cm^3	Thickness, in.	Ablator weight, lb/ft^2	Time for 400°F backface temp. rise, min.
SLA-561 (superlight ablator)	0.23	0.526	0.60	4.70
SLA-220 (rf-transparent ablator)	0.25	0.488	0.635	2.20
MA-25s (sprayable silicone ablator)	0.50	0.236	0.615	1.15
Porous Teflon	0.71	0.167	0.615	0.92

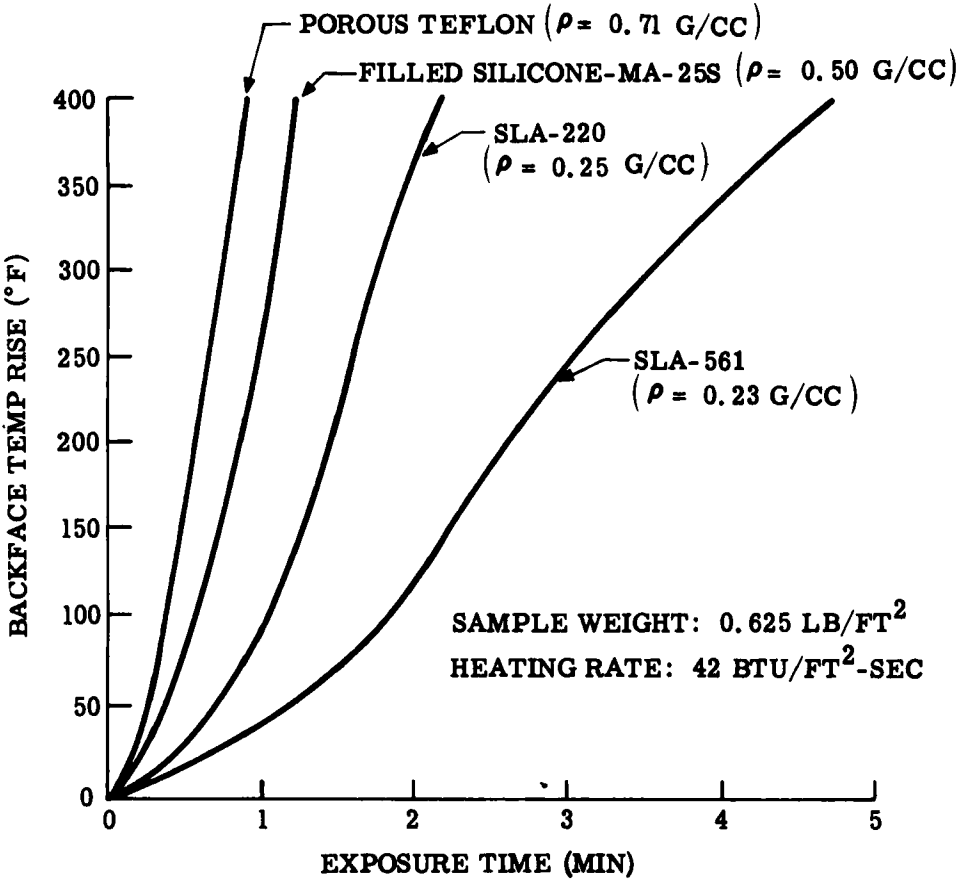

Fig. 6. Back-face temperature rise of ablators during propane torch heating.

Samples of porous Teflon ablators (0.51, 0.61, and 0.71 g/cm^3 density), and of Martin Marietta SLA-561, a high-efficiency superlight ablator (non-rf-transparent [5]) were tested concurrently to provide a basis for comparison. All ablators were tested in several different thicknesses in order to establish curves of ablator back-face temperature rise as a function of ablator weight (Figs. 7 and 8). Test conditions are described in Table 3.

SLA-220 tested at 6 Btu/ft^2-sec registered only slight surface recession (0.015 in. or less), and, in a number of instances, negative surface recession (growth) occurred. Silicone ablators tend to swell during resin pyrolysis, and later they undergo shrinkage during formation of a fully matured

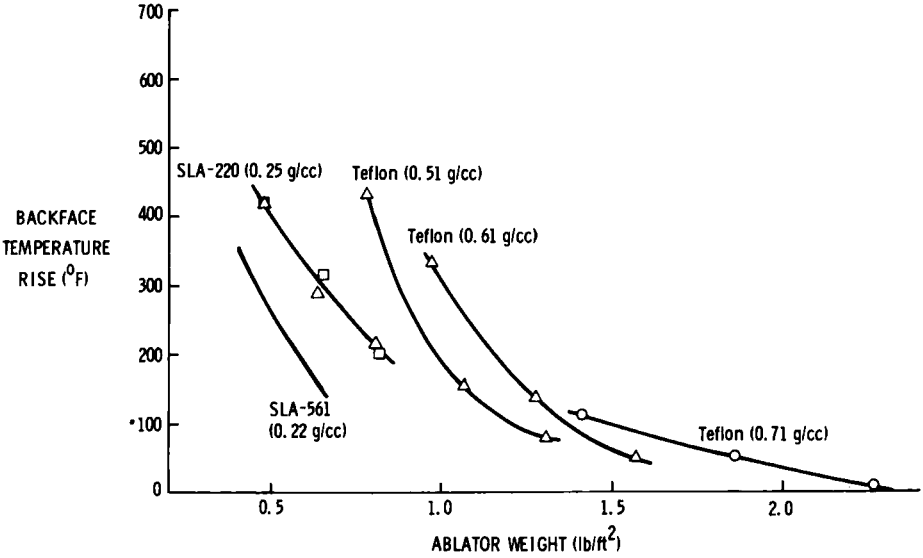

Fig. 7. Variation of back-face temperature rise with ablator weight for samples tested for 250 sec at 6 Btu/ft^2-sec.

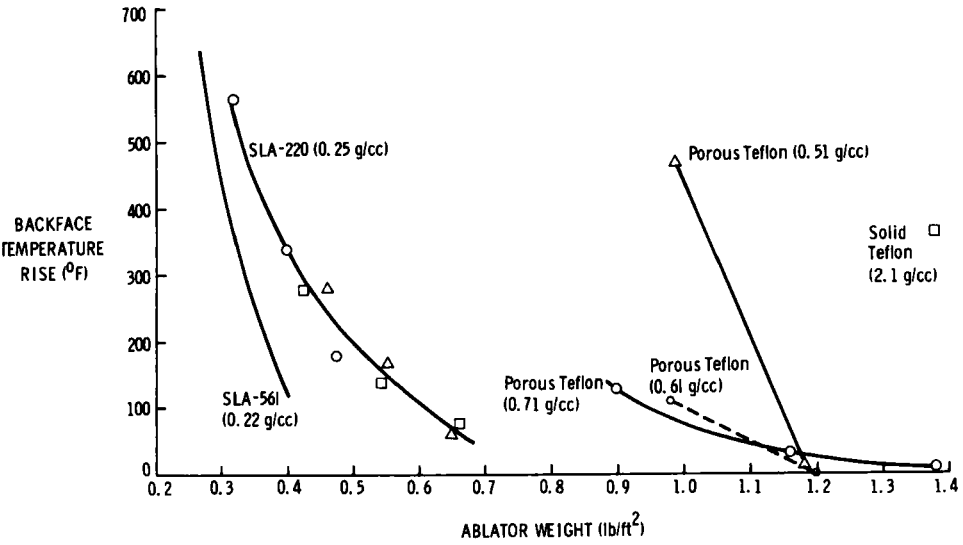

Fig. 8. Variation of back-face temperature rise with ablator weight for samples tested for 50 sec at 60 Btu/ft^2-sec.

Table 3. Plasma Arc Test Conditions

	Low heating rate	High heating rate
Heating rate, Btu/ft^2-sec	6.2	58.1
Enthalpy, Btu/lb	2520	7020
Stagnation pressure, atm	0.0034	0.0105
Exposure time, sec	250	50
Test gas	28% CO_2–72% N_2 (by weight)	

char. These phenomena rather than loss of surface material accounted for the small observed surface recessions. Exposure of SLA-220 for 50 sec at 60 Btu/ft^2-sec resulted predominantly in growth. The surface of SLA-220 after plasma arc exposure was dark grey to black, indicating carbon deposition near the outer surface. Samples tested for 50 sec at 60 Btu/ft^2-sec were substantially darker than samples exposed for 250 sec at 6 Btu/ft^2-sec. The thickness of the dark char layer was less than 1/16 in. in samples tested at 6 Btu/ft^2-sec, while samples tested at 60 Btu/ft^2-sec developed a dark char of 1/8- to 1/4-in. thickness despite the shorter exposure time. The porous Teflon samples, in contrast, did not form a char layer but underwent recession due to depolymerization. Surface recessions after 250 sec at 6 Btu/ft^2-sec were 0.340, 0.285, and 0.235 in. for the 0.51-, 0.60-, and 0.71-g/cm^3-density materials, respectively. For the 50-sec exposure at 60 Btu/ft^2-sec, the corresponding recessions were 0.335, 0.280, and 0.245 in. The curves of back-face temperature rise vs. ablator weight (Figs. 7 and 8) show that SLA-220 is less efficient than SLA-561, a superlight carbon char-forming ablator. However, when rf-transparency is required, SLA-220 can maintain a given back-face temperature at a substantial weight saving compared with porous Teflon.

THERMAL PROPERTIES

Thermal properties which have been measured include thermal conductivity, thermal expansion, and specific heat. Test results for SLA-220, porous Teflon, and SLA-561 are summarized in Table 4. Thermal

conductivity tests (Fig. 9) were conducted in a guarded hot-plate apparatus, using 9-in.-diam test samples. The average thermal conductivity of SLA-220 between 100 and 400°F was found to be approximately 50% higher than that of SLA-561. The corresponding conductivities of the porous Teflon materials (0.51 and 0.71 g/cm^3 densities) fell between the values for the superlight ablators with the higher-density Teflon exhibiting the higher conductivity.

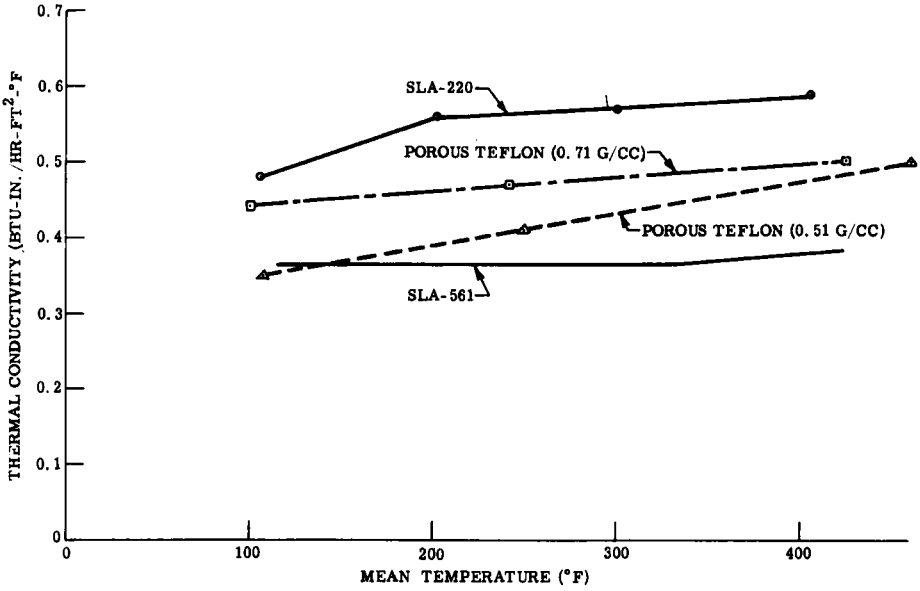

Fig. 9. Thermal conductivity of low-density ablators.

Specific heat values were measured in a steam jacket drop calorimeter and therefore represent an average between ambient temperature and 212°F. The value for SLA-220 reflects its high silica content, while the higher value for SLA-561 is due to the high organic content of that ablator. The value for Teflon listed in Table 4 is that reported by du Pont [8].

Thermal expansion of the superlight ablators was measured in a quartz tube dilatometer between room temperature and -320°F. Expansion data were recorded for three samples of each material while cooling from ambient to -320°F and also as the sample temperature returned to ambient. The thermal expansion of SLA-220 is not linear with temperature but

Table 4. Thermal Properties

Material	Density, g/cm^3	Thermal conductivity Btu-in./hr-ft^2-°F (Temperature span).	Specific heat, Btu/lb-°F	Coefficient of linear thermal expansion, in./in./°F (temperature span)
SLA-220	0.25	0.55 (avg. value) (100–400°F)	0.234	1.16×10^{-5} (0 to -250°F)
Porous Teflon	0.51	0.42 (avg. value) (100–460°F)	0.25	5.5×10^{-5} (73 to 140°F)
Porous Teflon	0.71	0.47 (avg. value) (100–420°F)	0.25	5.5×10^{-5} (73 to 140°F)
SLA-561	0.225	0.36 (100–450°F)	0.30	2.17×10^{-5} (73 to -200°F)

rather increases as temperature is reduced. However, since the expansion curves for SLA-220 do not deviate extensively from linearity, an average coefficient of expansion can be approximated. The value listed in Table 4 represents the average of the coefficients for the cooling and heating portions of the test. The coefficient of expansion for Teflon listed in Table 4 is that reported by du Pont [8].

MECHANICAL PROPERTIES

Tensile properties of SLA-220 and of porous Teflon ablators were determined over the temperature span of +200 to -200°F. Test coupons were dumbbell-shaped specimens, 1.5 in. wide X 9 in. long X 3/8 in. thick with a 0.5-in.-wide X 2.25-in.-long gauge section. Samples were instrumented with a slide wire extensometer and pulled to failure in tension. Elongation was measured optically over a 2-in. gauge length. Specimens tested at high and low temperatures were soaked for 1 hr at the test temperature prior to loading. SLA-220 coupons were also tested in compression (2.5-in.-diam X 1-in.-high cylinder), bearing (1-in.-diam steel rod, bearing on 2.5-in.-diam cylinder), and flexure (four-point loading). Room temperature strength values for SLA-220 are listed in Table 5. The tensile strength of SLA-220 was found to be 83 psi. The corresponding strengths of porous Teflon were 49, 85, and 152 psi for the 0.51-, 0.61-, and 0.71-g/cm^3-density materials, respectively.

Figure 10 shows typical tensile stress-strain curves for SLA-220. The curves exhibit a straight-line portion at most test temperatures; consequently, a modulus of elasticity can be calculated.

Table 5. Mechanical Properties of SLA-220 at Room Temperature

	Strength, psi	Modulus, psi	Elongation, %
Tension	83	1810	5.9
Flexure	150	3700	–
Compression	112	1900	–
Bearing	160	–	–

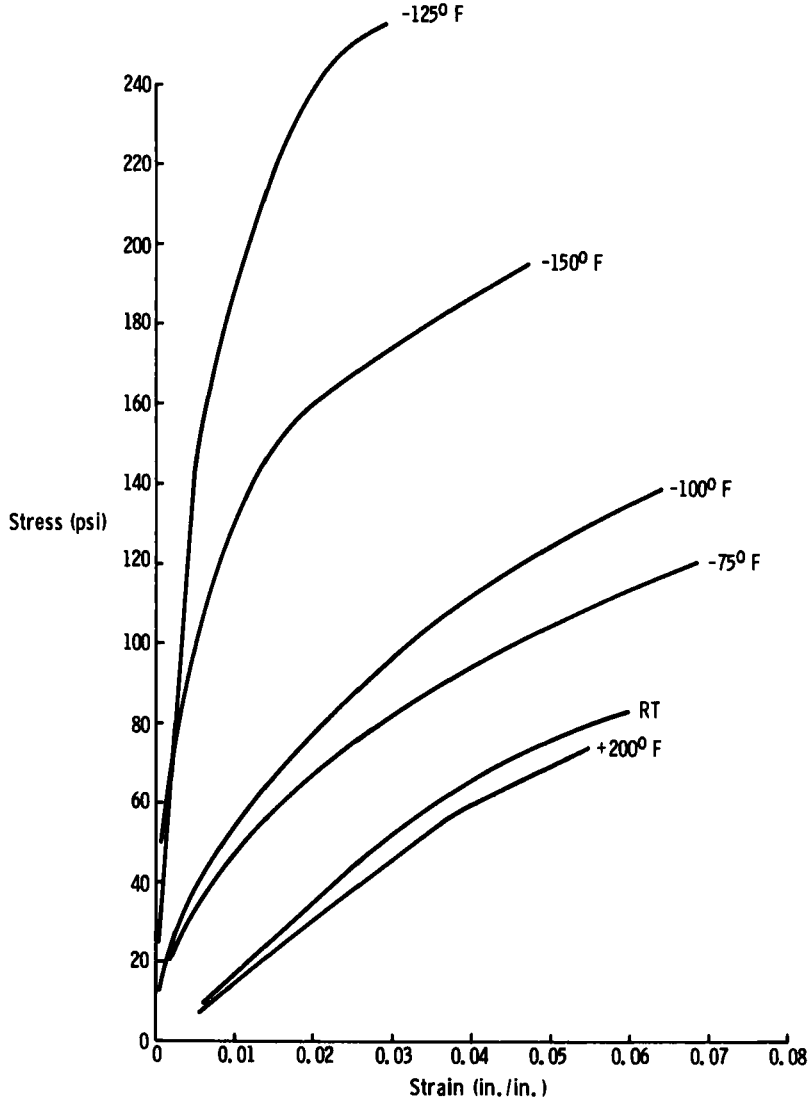

Fig. 10. Stress-strain curves for SLA-220 (series I).

Modulus values increased from 1300 psi at +200°F to 8220 psi at -125°F and then dropped to 3920 psi at -150°F. Variation in tensile strength and in elongation at failure with temperature is shown in Fig. 11. Initially, the low-temperature tests of SLA-220 were only intended to cover the temperature range of +200 to -150°F. When results showed that the curve of tensile properties vs. temperature was discontinuous at -125°F, it was deemed necessary to generate additional data over the temperature span of -125 to -200°F. Consequently, a second series of SLA-220 specimens was prepared and tested. Series II specimens were prepared in the same manner as series I specimens and their densities differed by less than 2%. Series I and II specimens were tested at three common temperatures, ambient, -125, and -150°F.

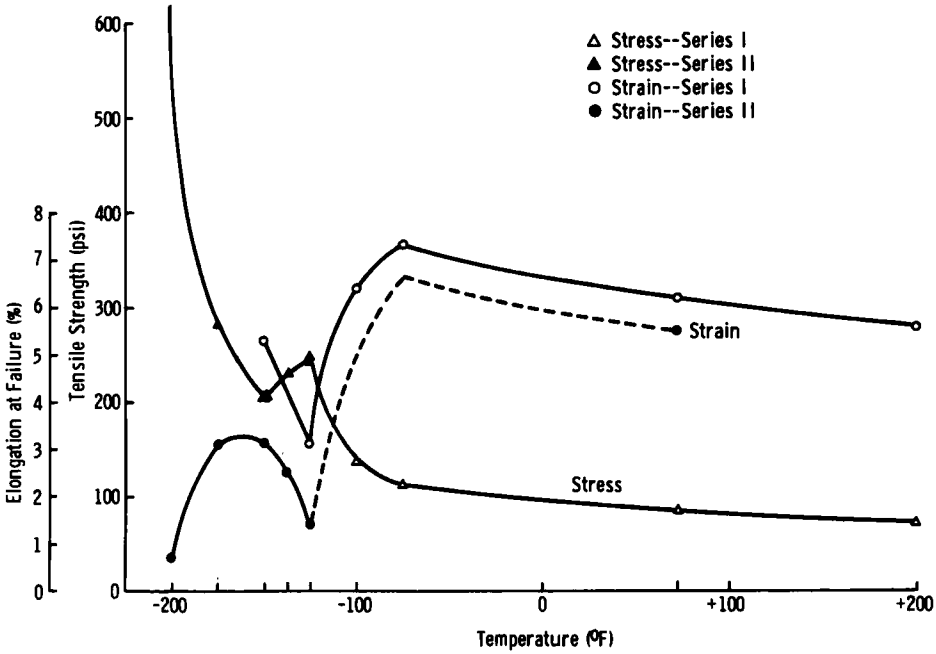

Fig. 11. Variation of tensile properties of SLA-220 with temperature.

As shown in Fig. 11, the two specimen groups developed virtually identical tensile strengths, but the elongation at failure of series II material was appreciably lower than that of series I material. No cause for this discrepancy has been found. The variation of SLA-220 tensile strength with temperature

has been represented in Fig. 11 by a single curve. However, separate curves for series I and series II materials had to be drawn to represent the variation of elongation at failure with temperature.

The tensile properties of SLA-220 exhibited contrasting temperature dependencies in different temperature regions, as summarized in Table 6.

Table 6.

Temperature range, °F	Strain at failure	Tensile strength
+200 to −75°	Gradual increase	Gradual increase
−75 to −125°	Sharp decline	Sharp increase
−125 to −150°	Sharp increase	Moderate decrease
−150 to −175°	Peak of curve	Moderate increase
−175 to −200°	Sharp decrease	Sharp increase

Expansion and penetration probe data (Fig. 12) derived for the SLA-220 resin system on a du Pont thermomechanical analyzer have established that the glass transition temperature of this resin is -128°F (-78°C). It can therefore be concluded that the inversion in the slope of the tensile properties vs. temperature curve at -125°F is associated with the glass transition temperature of the resin.

WEIGHT LOSS CHARACTERISTICS

Studies were conducted to determine the weight loss of SLA-220 under conditions simulating sterilization and space (vacuum and temperature) exposure. Disks of SLA-220, 2.5 in. in diam × 0.5 in. thick and weighing approximately 11 g each, were exposed for 92 hr at 135°C (275°F) in nitrogen. Similar disks were also exposed for 96 hr at 160°F in vacuum. Three SLA-220 formulations were investigated: standard SLA-220, SLA-220 containing a modified catalyst system, and SLA-220 containing a methyl-phenyl siloxane rather than a high-methyl siloxane.

The samples were allowed to cool after the exposure and were then weighed and measured. The data presented in Table 7 show that only slight weight and dimensional changes occurred. Weight loss was of the order of 1% or less while dimensional changes were less than 0.10%. Weight loss of the resin-modified SLA-220 was almost twice that of the standard SLA-220 ablator or of the catalyst-modified SLA-220. For all

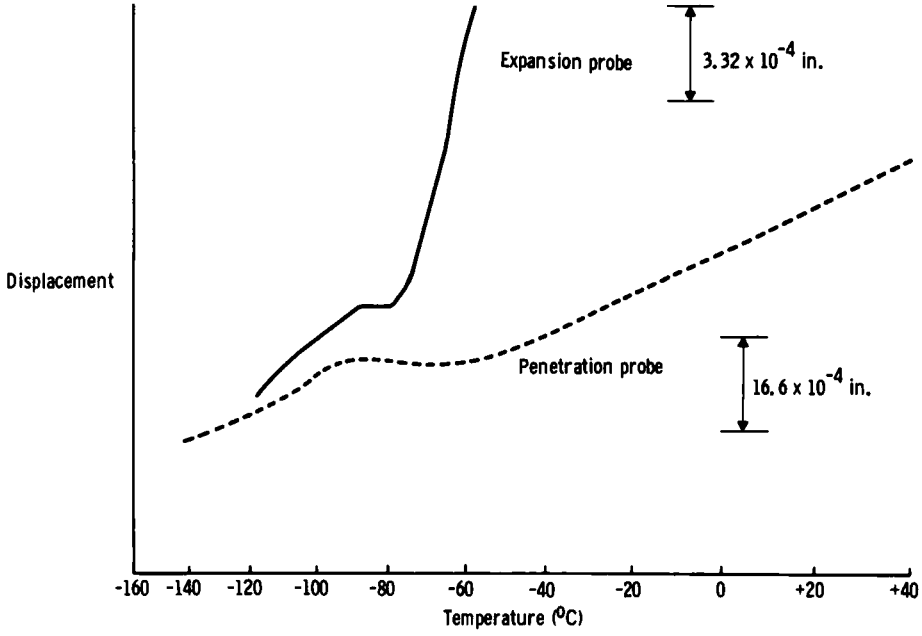

Fig. 12. Penetration and expansion traces (du Pont thermomechanical analyzer) for silicone resin system used in SLA-220. Heating rate = 5°C/min.

three materials, the weight loss after 96 hr at 160°F in vacuum was only half that noted in the corresponding samples after the 92-hr exposure at 275°F in N_2. In addition, the vacuum exposure caused a slight dimensional shrinkage while the nitrogen exposure caused a slight dimensional expansion.

Following their respective exposures at 160 and 275°F, the samples were kept at ambient room conditions and periodically weighed and measured. The samples immediately began to regain part of the weight loss, and after approximately 100 hr their weights had stabilized, as shown in Fig. 13. For all practical purposes, the samples exposed at 160°F in vacuum did not change dimensionally during the recovery period. The samples exposed at 275°F in N_2, on the other hand, experienced slight shrinkage during the recovery period. When measured soon after cooling, following the 92-hr exposure at 275°F, the samples had registered dimensional expansion. The relaxation during the recovery period was such that the net dimensional change with respect to the original specimen dimension was shrinkage. Weight and dimensional changes (with respect to pre-exposure measurements)

Table 7. Weight and Dimensional Changes after Thermal Exposure

	Weight loss, %	Shrinkage, %	
		Diameter	Thickness
92 hr at 275°F in N_2			
SLA-220	0.60	-0.07 (growth)	-0.05 (growth)
Modified SLA-220 (catalyst)	0.57	-0.04 (growth)	-0.01 (growth)
Modified SLA-220 (resin)	1.11	0.01	-0.08 (growth)
96 hr at 160°F in vacuum			
SLA-220	0.30	0.06	0.03
Modified SLA-220 (catalyst)	0.31	0.04	0.05
Modified SLA-220 (resin)	0.63	0.07	0.03

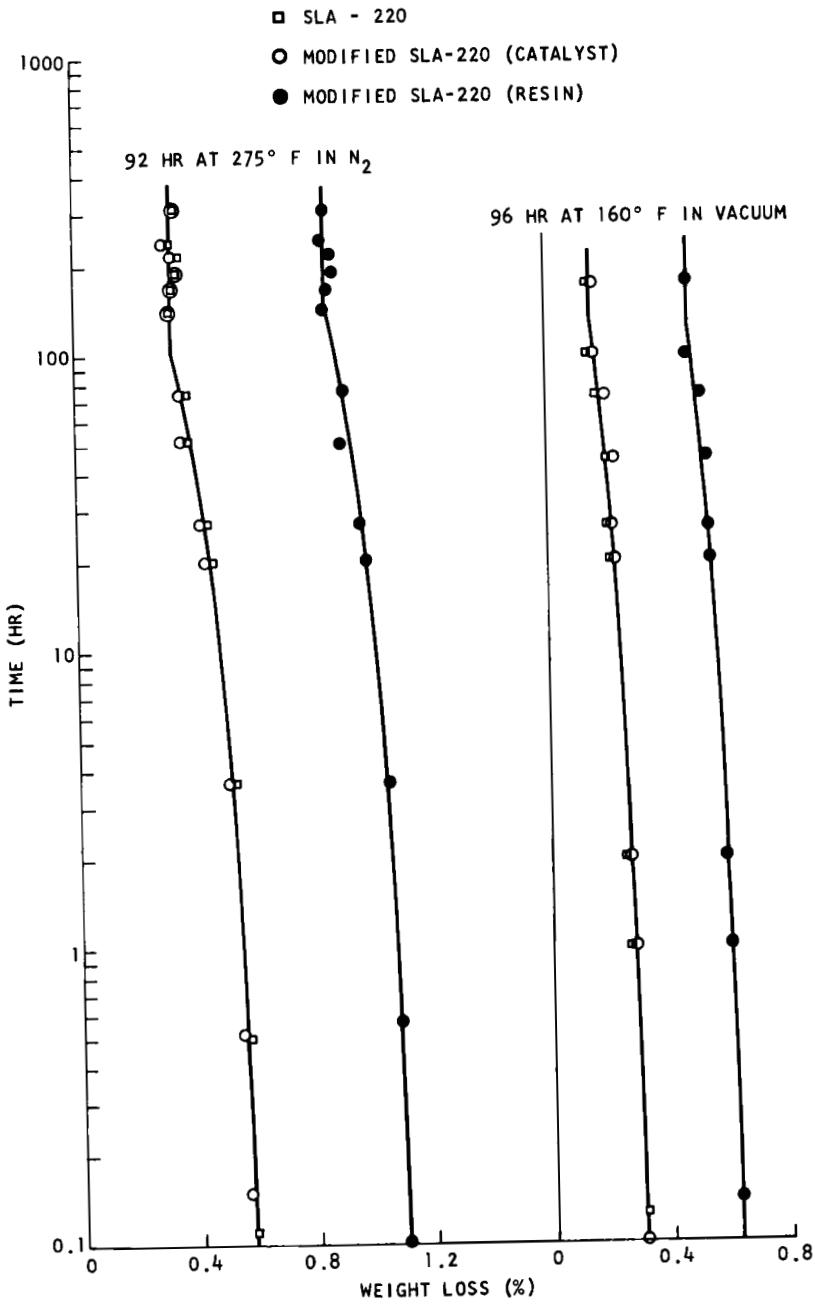

Fig. 13. Weight recovery after elevated temperature exposure.

after a 200-hr recovery period are summarized in Table 8. Since these changes are quite minute, they should have practically no effect on the mechanical or ablative performance of SLA-220 after sterilization or vacuum exposure.

To determine the rate of weight loss of SLA-220 during elevated temperature exposure, an isothermal weight loss study was carried out in the Martin Marietta TGA apparatus. An 812-mg sample of SLA-220 was kept in the TGA furnace at 140°C under a flow of argon, and weight loss was monitored continuously. It took approximately 0.1 hr for the furnace temperature to reach 140°C. At that point, a weight loss of 0.26% had occurred. Isothermal weight loss at 140°C was then measured for an additional 42 hr. The weight loss can be represented by a straight line on a $\log_{10}$ time versus per cent weight loss plot (Fig. 14) and can be mathematically expressed by:

$$\% \text{ weight loss} = 0.50 + 0.25 \log_{10} t$$

where t is given in hours.

After 42 hr at 140°C, the furnace was allowed to cool to room temperature, then the argon flow was shut off and the recovery of weight loss was monitored with the sample in the furnace in an ambient environment. The weight recovery for the first 50 hr also forms a straight line on a $\log_{10}$ t versus per cent weight loss plot (Fig. 14), which can be expressed by:

$$\% \text{ weight loss} = 0.75 - 0.15 \log_{10} t$$

After a recovery period of 50 hr, the net weight loss was approximately 0.50% and appeared to have stabilized at that point.

CONCLUSIONS

SLA-220, a silica-filled silicone ablator of 0.25 g/cm^3 density exhibits acceptable radio frequency signal transmission after ablation. Signal attenuation after exposure to heat fluxes of 6 and 11.4 Btu/ft^2-sec is slight, and, although attenuation increases with heating rate, dB losses are less than 6 dB for exposures up to 60 Btu/ft^2-sec. Further investigations are required to establish the effects of heating rate, length of exposure, and type of heating on char formation and signal attenuation. In addition, it is necessary to check transmission during ablation and immediately upon cessation of heating while the ablator char is hot.

Density and thermal conductivity of SLA-220 are higher than those of

Table 8. Weight and Dimensional Changes Following Recovery after Thermal Exposure

	Weight loss, %	Shrinkage, %	
		Diameter	Thickness
92 hr at 275°F in N_2 and 200 hr at room temperature			
SLA-220	0.34	0.14	0.04
Modified SLA-220 (catalyst)	0.33	0.14	0.06
Modified SLA-220 (resin)	0.85	0.05	0.02
96 hr at 160°F in vacuum and 200 hr at room temperature			
SLA-220	0.14	0.10	0.02
Modified SLA-220 (catalyst)	0.16	0.07	0.04
Modified SLA-220 (resin)	0.48	0.13	0.01

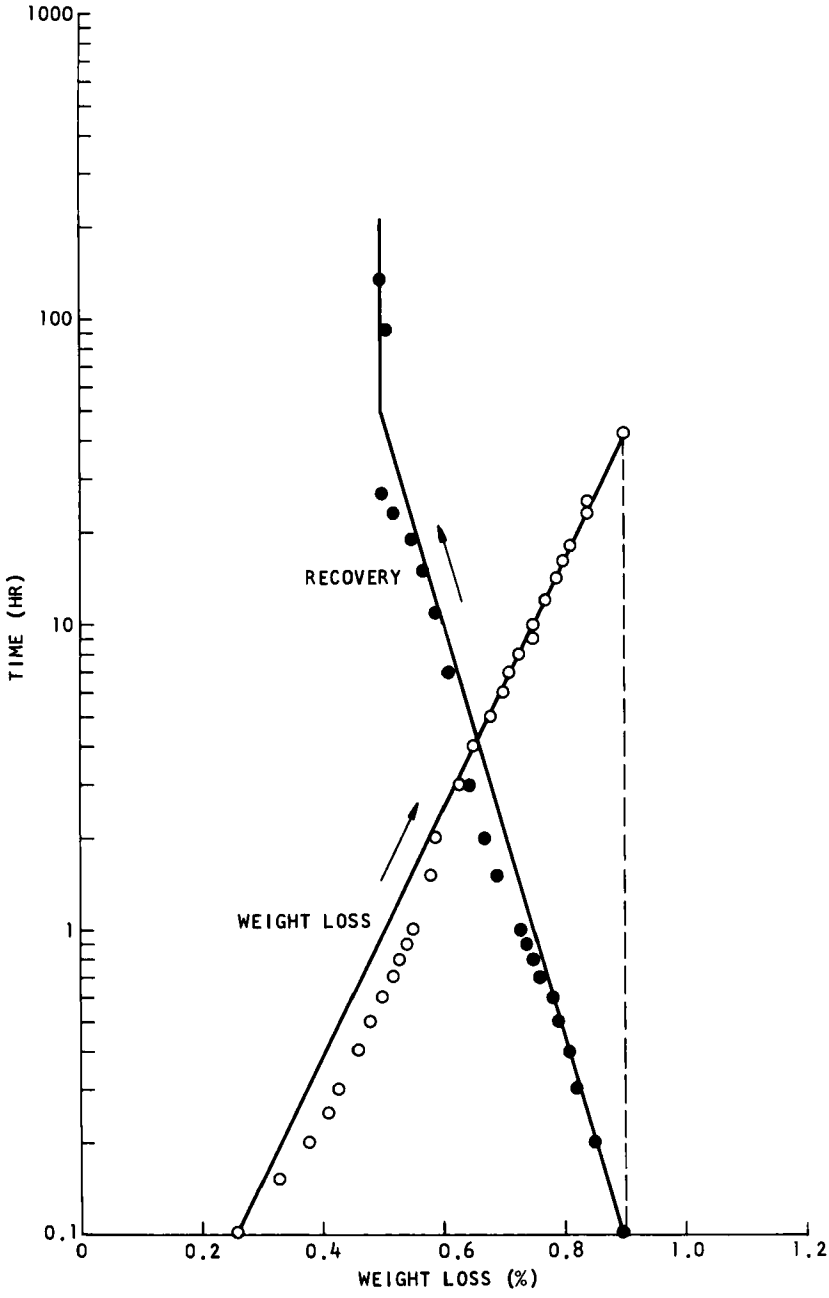

Fig. 14. Isothermal weight loss of SLA-220 at 140°C (284°F) in argon.

SLA-561, and the specific heat of SLA-220 is lower. This is reflected in the lower ablative efficiency of SLA-220 when compared with the superlight SLA-561 composition. However, SLA-220 develops a considerably higher ablative efficiency than porous Teflon. While SLA-220 undergoes practically no surface recession during heating to 60 Btu/ft^2-sec, porous Teflon exhibits significant recession at these heating rates.

REFERENCES

[1] S. L. Channon and W. T. Berry, "Status of Reentry Vehicle Heatshields," presented at AIAA/ASME 8th Structures, Structural Dynamics and Materials Conf., Palm Springs, Calif., March 29-31, 1967.

[2] W. E. Welsh, D. Leeds, K. Starner, and J. Slaughter, *SSD-TR-66-35*, January 1966.

[3] E. L. Strauss, *Soc. Automotive Engr. Trans.*, 1967, pp. 293-304.

[4] L. F. Vosteen, "Heat-Shield Materials Development for Voyager," presented at 3rd Intern. Symp. High Temperature Tech., Asilomar, Calif., September 17-20, 1967.

[5] E. L. Strauss, *J. Spacecraft and Rockets*, 4, 1304-1309 (1967).

[6] R. G. Nagler, "The Mars Transit and Entry Environment—A New Problem for Heat Shields," Proc. Reprint, 13th Annual Tech. Meeting, Inst. Environ. Sci., 1967.

[7] J. Meltzer, J. Rosoff, J. I. Slaughter, and J. Sterhardt, "Structure and Materials Aspects of the Prime Flight Test Vehicle," presented at AIAA/ASME 7th Structures and Materials Conf., Cocoa Beach, Fla., April 1966.

[8] *Teflon Tetrafluoroethylene Resin*, E. I. du Pont de Nemours & Co., Wilmington, Dela.

Accepted by editor December 24, 1968
Received for publication January 3, 1969